

Convex Environmental Contours

Arne Bang Huseby
University of Oslo, Norway

Erik Vanem
DNV GL, Norway

Christian Agrell
DNV GL, Norway

Andreas Hafver
DNV GL, Norway

Abstract

Environmental contours are widely used as a basis for e.g., ship design, especially in early design phases. The traditional approach to such contours is based on the well-known Rosenblatt transformation. Here we focus on convex contours estimated using Monte Carlo based methods. It is well-known that contours constructed with such methods typically have certain irregularities. In particular, the sets bounded by the estimated contours appear to be convex. However, when the curves are investigated more closely, they include a large number of small loops. In the present paper we provide a precise condition for convexity, and propose a smoothing method which can be used to eliminate the loops. The methods are illustrated by a numerical example.

ENVIRONMENTAL CONTOURS; MONTE CARLO METHODS

1 Introduction

Environmental contours are widely used as a basis for e.g., ship design. Such contours are typically used in early design when the strength and failure properties of the object under consideration are not known. An environmental contour describes the tail properties of some relevant environmental variables, and is used as input to the design process. See Haver (1987), Baarholm et al. (2010), Ditlevsen (2002), Moan (2009) and Jonathan et al. (2011). The methodology for constructing environmental contours were introduced by Winterstein et al. (1993) and Haver and Winterstein (2009). The process starts out by constructing a contour for two independent standard normally distributed variables. This contour is then transformed to the environmental space using the inverse Rosenblatt transformation introduced in Rosenblatt (1952). As pointed out in Huseby et al. (2013) the probabilistic properties of the contour is typically not preserved under this transformation. Hence, the resulting contour may need to be adjusted in order to get the desired exceedance probability. Huseby et al. (2013) also presented an alternative approach where environmental contours are constructed using Monte Carlo simulation. For a similar approach to a related problem see Ottesen and Aarstein (2006). Improved methods are found in Huseby et al. (2015a) and Huseby et al. (2015b).

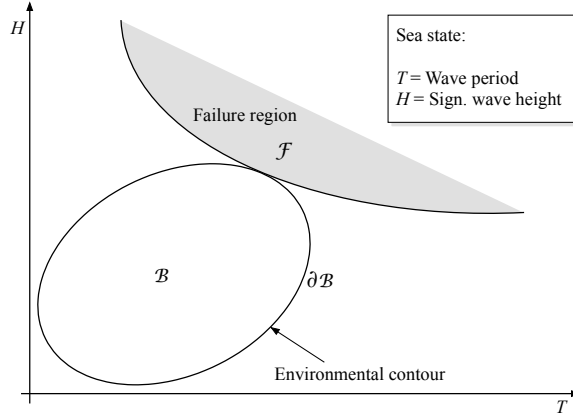


Figure 2.1: An environmental contour and a failure region.

A challenge with Monte Carlo based methods is that in order to obtain stable results it may be necessary to run a large number of simulations. In Huseby et al. (2015b) this issue was addressed by using importance sampling. This methodology has later been refined further. Still, even though the resulting contours are fairly precise, a closer examination of the curves reveals certain irregularities. In the present paper we study this problem in detail, and show why these irregularities occur. Based on the theoretical results we also propose a simple smoothing method for removing these irregularities.

2 Basic concepts

Let $(T, H) \in \mathbb{R}^2$ be a vector of environmental variables where e.g.,:

$$\begin{aligned} T &= \text{Wave period} \\ H &= \text{Significant wave height} \end{aligned}$$

The distribution of (T, H) is assumed to be absolutely continuous with respect to the Lebesgues measure in \mathbb{R}^2 .

An *environmental contour* is defined as the boundary of a compact¹ set $\mathcal{B} \subseteq \mathbb{R}^2$ and denoted $\partial\mathcal{B}$. To avoid pathological cases we always assume that these sets have a *non-empty* interior. In particular, sets containing just a *single point* will not be considered.

During the design phase of some structure of interest the environmental contour can be used to identify conditions which the structure should be able to withstand. That is, if $(T, H) \in \mathcal{B}$, the structure should function normally. Consequently, the environmental contour $\partial\mathcal{B}$ represents the most severe or extreme conditions that the structure should be able to handle, and the points on this contour represent possible design requirements for the structure.

The *failure region* $\mathcal{F} \subseteq \mathbb{R}^2$ of a structure is the set of states where the structure fails. See Figure 2.1. For a given environmental contour \mathcal{B} we say that the design requirements are satisfied if and only if $\mathcal{F} \cap \mathcal{B} \subseteq \partial\mathcal{B}$. If the set \mathcal{B} is large, this implies that the structure will be subject to very strict requirements. As a result, the probability of failure, i.e., the probability that $(T, H) \in \mathcal{F}$ is small.

¹A set is *compact* if it is closed and bounded

In the design phase the exact shape of the failure region of a structure is typically unknown. It may still be possible to argue that the failure region belongs to a certain family denoted by \mathcal{E} . We then say that the design requirements are satisfied if and only if $\mathcal{F} \cap \mathcal{B} \subseteq \partial\mathcal{B}$ for all $\mathcal{F} \in \mathcal{E}$.

The *exceedance probability* of \mathcal{B} with respect to \mathcal{E} is defined as:

$$P_e(\mathcal{B}, \mathcal{E}) = \sup_{\mathcal{F} \in \mathcal{E}} \{P[(T, H) \in \mathcal{F}]\}.$$

The exceedance probability is an upper bound on the failure probability of the structure assuming that the true failure region is a member of the family \mathcal{E} . For a given target exceedance probability $p_e \in (0, 0.5)$ our goal is to find a minimal set \mathcal{B} such that:

$$P_e(\mathcal{B}, \mathcal{E}) \leq p_e. \quad (2.1)$$

If the set \mathcal{B} satisfies (2.1), then $\partial\mathcal{B}$ is said to be a *valid* environmental contour.

A failure region $\mathcal{F} \in \mathcal{E}$ is said to be *maximal* if there does not exist a region $\mathcal{F}' \in \mathcal{E}$ such that $\mathcal{F} \subset \mathcal{F}'$. The family of maximal regions in \mathcal{E} is denoted by \mathcal{E}^* . If $\mathcal{F}_1, \mathcal{F}_2 \in \mathcal{E}$ and $\mathcal{F}_1 \subseteq \mathcal{F}_2$, we obviously have:

$$P[(T, H) \in \mathcal{F}_1] \leq P[(T, H) \in \mathcal{F}_2].$$

From this it follows that:

$$\begin{aligned} P_e(\mathcal{B}, \mathcal{E}) &= \sup_{\mathcal{F} \in \mathcal{E}} \{P[(T, H) \in \mathcal{F}]\} \\ &= \sup_{\mathcal{F} \in \mathcal{E}^*} \{P[(T, H) \in \mathcal{F}]\}. \end{aligned}$$

3 Convex environmental contours

It is often natural to assume that a failure region is *convex*. This means that if the structure fails at two distinct points (t_1, h_1) and (t_2, h_2) , then it also fails for all states on the straight line between these points. If the contour is convex as well, this implies that the maximal failure regions are halfspaces. See Figure 3.1 where Π is a supporting hyperplane of the convex set \mathcal{B} , while Π^+ is a supporting halfspace of \mathcal{B} . The set Π^- is the halfspace separated from Π^+ by the hyperplane Π . We say that Π^- as the halfspace *opposite* to the supporting halfspace Π^+ , and observe that $\mathcal{B} \subseteq \Pi^-$.

In the remaining parts of this paper we only consider contour sets \mathcal{B} which are *compact* and *convex*. Furthermore, we assume that all the sets in \mathcal{E} are *convex*. For a given compact and convex set \mathcal{B} we introduce the following families of sets:

- $\mathcal{P}(\mathcal{B})$ = The family of supporting hyperplanes of \mathcal{B} ,
- $\mathcal{P}^+(\mathcal{B})$ = The family of supporting halfspaces of \mathcal{B} ,
- $\mathcal{P}^-(\mathcal{B})$ = The family of halfspaces opposite to supporting halfspaces of \mathcal{B}

By using well-known results from convexity theory, it is easy to show the following result:

Proposition 3.1 *Let $\mathcal{B} \subset \mathbb{R}^2$ be a compact and convex set, and let \mathcal{E} be the family of convex sets such that $\mathcal{F} \cap \mathcal{B} \subseteq \partial\mathcal{B}$ for all $\mathcal{F} \in \mathcal{E}$. Then $\mathcal{E}^* = \mathcal{P}^+(\mathcal{B})$, and hence:*

$$P_e(\mathcal{B}, \mathcal{E}) = \sup_{\Pi^+ \in \mathcal{P}^+(\mathcal{B})} \{P[(T, H) \in \Pi^+]\}. \quad (3.1)$$

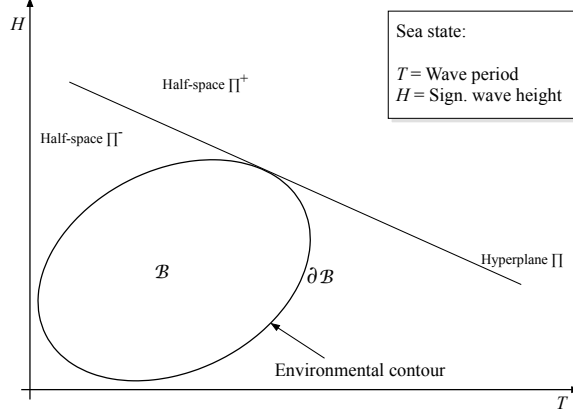


Figure 3.1: Supporting hyperplane and halfspaces

Moreover, the set \mathcal{B} can be expressed as:

$$\mathcal{B} = \bigcap_{\Pi^- \in \mathcal{P}^-(\mathcal{B})} \Pi^-. \quad (3.2)$$

The families $\mathcal{P}(\mathcal{B})$, $\mathcal{P}^+(\mathcal{B})$ and $\mathcal{P}^-(\mathcal{B})$ can be expressed in a more explicit form. In order to explain how this can be done, we start out by letting $\theta \in [0, 2\pi)$, and define:

$$B(\mathcal{B}, \theta) = \sup_{(t,h) \in \mathcal{B}} [t \cos(\theta) + h \sin(\theta)] \quad (3.3)$$

We also introduce :

$$\begin{aligned} \Pi(\mathcal{B}, \theta) &= \{(t, h) : t \cos(\theta) + h \sin(\theta) = B(\mathcal{B}, \theta)\} \\ \Pi^+(\mathcal{B}, \theta) &= \{(t, h) : t \cos(\theta) + h \sin(\theta) \geq B(\mathcal{B}, \theta)\}, \\ \Pi^-(\mathcal{B}, \theta) &= \{(t, h) : t \cos(\theta) + h \sin(\theta) \leq B(\mathcal{B}, \theta)\}. \end{aligned}$$

Since \mathcal{B} is assumed to be compact, it follows that \mathcal{B} is bounded, and thus, $B(\mathcal{B}, \theta)$ must be finite. Moreover, by the definition of $B(\mathcal{B}, \theta)$ it follows that:

$$t \cos(\theta) + h \sin(\theta) \leq B(\mathcal{B}, \theta), \quad \text{for all } (t, h) \in \mathcal{B}.$$

Finally, since \mathcal{B} is compact, \mathcal{B} is closed as well. Thus, there must exist at least one point $(t_0, h_0) \in \mathcal{B}$ such that:

$$t_0 \cos(\theta) + h_0 \sin(\theta) = B(\mathcal{B}, \theta)$$

From this it follows that $\Pi(\mathcal{B}, \theta) \in \mathcal{P}(\mathcal{B})$, $\Pi^+(\mathcal{B}, \theta) \in \mathcal{P}^+(\mathcal{B})$ and $\Pi^-(\mathcal{B}, \theta) \in \mathcal{P}^-(\mathcal{B})$.

Assume conversely that $\Pi \in \mathcal{P}(\mathcal{B})$, and let Π^+ and Π^- be the corresponding supporting and opposite halfspaces separated by Π . Then Π , Π^+ and Π^- can be expressed as follows:

$$\begin{aligned} \Pi &= \{(t, h) : ta_1 + ha_2 = b\}, \\ \Pi^+ &= \{(t, h) : ta_1 + ha_2 \geq b\}, \\ \Pi^- &= \{(t, h) : ta_1 + ha_2 \leq b\} \end{aligned}$$

for suitable real numbers a_1 , a_2 and b . Without loss of generality we may assume that a_1 and a_2 are *normalized* such that $a_1^2 + a_2^2 = 1$. Then it follows that there exists a $\theta \in [0, 2\pi)$ such that $a_1 = \cos(\theta)$ and $a_2 = \sin(\theta)$.

Since Π^+ is a supporting halfspace of \mathcal{B} , we must have:

$$t \cos(\theta) + h \sin(\theta) \leq b, \quad \text{for all } (t, h) \in \mathcal{B},$$

and

$$t_0 \cos(\theta) + h_0 \sin(\theta) = b, \quad \text{for some } (t_0, h_0) \in \mathcal{B},$$

From this it follows that:

$$b = \sup_{(t,h) \in \mathcal{B}} [t \cos(\theta) + h \sin(\theta)] = B(\mathcal{B}, \theta),$$

implying that $\Pi = \Pi(\mathcal{B}, \theta)$, $\Pi^+ = \Pi^+(\mathcal{B}, \theta)$ and $\Pi^- = \Pi^-(\mathcal{B}, \theta)$. The following proposition summarizes these findings:

Proposition 3.2 *Let $\mathcal{B} \subset \mathbb{R}^2$ be a compact and convex set. Then we have:*

$$\begin{aligned} \mathcal{P}(\mathcal{B}) &= \{\Pi(\mathcal{B}, \theta) : \theta \in [0, 2\pi)\}, \\ \mathcal{P}^+(\mathcal{B}) &= \{\Pi^+(\mathcal{B}, \theta) : \theta \in [0, 2\pi)\}, \\ \mathcal{P}^-(\mathcal{B}) &= \{\Pi^-(\mathcal{B}, \theta) : \theta \in [0, 2\pi)\}. \end{aligned}$$

Furthermore, by combining Proposition 3.1 and Proposition 3.2 we also obtain the following result:

Proposition 3.3 *Let $\mathcal{B} \subset \mathbb{R}^2$ be a compact and convex set, and let \mathcal{E} be the family of convex sets such that $\mathcal{F} \cap \mathcal{B} \subseteq \partial \mathcal{B}$ for all $\mathcal{F} \in \mathcal{E}$. Then we have:*

$$P_e(\mathcal{B}, \mathcal{E}) = \sup_{\theta \in [0, 2\pi)} \{P[(T, H) \in \Pi^+(\mathcal{B}, \theta)]\}. \quad (3.4)$$

Moreover, the set \mathcal{B} can be expressed as:

$$\mathcal{B} = \bigcap_{\theta \in [0, 2\pi)} \Pi^-(\mathcal{B}, \theta) \quad (3.5)$$

An immediate consequence of this result is that the function B induces an *ordering* of compact and convex sets. More formally, we have the following result:

Proposition 3.4 *Let \mathcal{B}_1 and \mathcal{B}_2 be two compact and convex sets, and assume that:*

$$B(\mathcal{B}_1, \theta) \leq B(\mathcal{B}_2, \theta) \text{ for all } \theta \in [0, 2\pi).$$

Then $\mathcal{B}_1 \subseteq \mathcal{B}_2$.

Proof: If $B(\mathcal{B}_1, \theta) \leq B(\mathcal{B}_2, \theta)$ for all $\theta \in [0, 2\pi)$, this implies that:

$$\Pi^-(\mathcal{B}_1, \theta) \subseteq \Pi^-(\mathcal{B}_2, \theta) \text{ for all } \theta \in [0, 2\pi).$$

Hence, by the second part of Proposition 3.3 we get that:

$$\mathcal{B}_1 = \bigcap_{\theta \in [0, 2\pi)} \Pi^-(\mathcal{B}_1, \theta) \subseteq \bigcap_{\theta \in [0, 2\pi)} \Pi^-(\mathcal{B}_2, \theta) = \mathcal{B}_2 \blacksquare$$

Another consequence of Proposition 3.3 is that a compact and convex set $\mathcal{B} \subset \mathbb{R}^2$ is uniquely determined by the function $B(\mathcal{B}, \theta)$. Hence, the boundary $\partial\mathcal{B}$ can be reconstructed from this function as well. In order to study the relation between $B(\mathcal{B}, \theta)$ and $\partial\mathcal{B}$ further, the following result, first proved by Minkowski in 1896, is relevant:

Proposition 3.5 (Minkowski) *Let \mathcal{B} be a closed convex set. Then for every point $\mathbf{x} \in \partial\mathcal{B}$ there exists a hyperplane $\Pi \in \mathcal{P}(\mathcal{B})$ such that $\mathbf{x} \in \Pi$.*

By using Proposition 3.2 this result can be restated for compact convex sets in \mathbb{R}^2 as follows:

Proposition 3.6 *Let $\mathcal{B} \subset \mathbb{R}^2$ be a compact convex set. Then for every point $(t_0, h_0) \in \partial\mathcal{B}$ there exists a $\theta \in [0, 2\pi)$ such that $(t_0, h_0) \in \Pi(\mathcal{B}, \theta)$.*

This proposition indicates that it may be possible to construct a mapping from angles $\theta \in [0, 2\pi)$ to the points in $\partial\mathcal{B}$. In the general case, however, the relation between angles and boundary points is not straightforward. By the definition of $B(\mathcal{B}, \theta)$ it follows that for a given $\theta \in [0, 2\pi)$ there exists at least one point $(t_0, h_0) \in \mathcal{B}$ such that:

$$t_0 \cos(\theta) + h_0 \sin(\theta) = B(\mathcal{B}, \theta), \quad (3.6)$$

and this point must also be on the boundary of \mathcal{B} . However, (t_0, h_0) may not be the only boundary point which satisfies (3.6). As an example consider a case where \mathcal{B} is a convex polygon. If, for a given θ , the vector $(\cos(\theta), \sin(\theta))$ is orthogonal to, and pointing away from one of sides of \mathcal{B} , then the hyperplane $\Pi(\mathcal{B}, \theta)$ intersects with all the points on this side. On the other hand, for any $\theta' \neq \theta$, the corresponding supporting hyperplane $\Pi(\mathcal{B}, \theta')$ does not intersect with any of the points on this side (except possibly the endpoints). Hence, it is not possible to define a mapping where each angle $\theta \in [0, 2\pi)$ is mapped to a unique point $(t_0, h_0) \in \partial\mathcal{B}$.

In order to avoid such problems we assume that \mathcal{B} is *strictly* convex. That is, for any pair of distinct points $(t_1, h_1), (t_2, h_2) \in \mathcal{B}$, all the points on the line segment between (t_1, h_1) and (t_2, h_2) (except possibly the endpoints (t_1, h_1) and (t_2, h_2)) belong to the interior of \mathcal{B} . The following proposition essentially states that for strictly convex sets there exists a well-defined mapping from angles to boundary points.

Proposition 3.7 *Let $\mathcal{B} \subset \mathbb{R}^2$ be a compact and strictly convex set. Then for every angle $\theta \in [0, 2\pi)$ there exists a unique point $(t(\theta), h(\theta)) \in \partial\mathcal{B}$ such that $(t(\theta), h(\theta)) \in \Pi(\mathcal{B}, \theta)$.*

Proof: By the definition of $\Pi(\mathcal{B}, \theta)$ we know that there exists at least one point $(t_1, h_1) \in \partial\mathcal{B}$ such that $(t_1, h_1) \in \Pi(\mathcal{B}, \theta)$. Assume, for a contradiction that there exists another boundary point (t_2, h_2) , different from (t_1, h_1) , which also belongs to the hyperplane $\Pi(\mathcal{B}, \theta)$. Since $\Pi(\mathcal{B}, \theta)$ is convex, all the points on the line segment between (t_1, h_1) and (t_2, h_2) also belong to $\Pi(\mathcal{B}, \theta)$. However, since \mathcal{B} is assumed to be strictly convex, the points on the line segment between (t_1, h_1) and (t_2, h_2) are elements of the interior of \mathcal{B} , which contradicts that $\Pi(\mathcal{B}, \theta)$ is a supporting hyperplane of \mathcal{B} . Hence, we conclude that $(t_1, h_1) \in \partial\mathcal{B}$ is the only boundary point which intersects with $\Pi(\mathcal{B}, \theta)$, and we define $(t(\theta), h(\theta))$ to be this point \blacksquare

If the function $B(\mathcal{B}, \cdot)$ is differentiable, the mapping from angles to boundary points is given by the following explicit formula:

Proposition 3.8 *Let $\mathcal{B} \subset \mathbb{R}^2$ be a compact and strictly convex set, and assume that $B(\mathcal{B}, \cdot)$ defined by (3.3) is differentiable. Then the boundary of \mathcal{B} can be expressed as:*

$$\partial\mathcal{B} = \{(t(\theta), h(\theta)) : \theta \in [0, 2\pi)\}$$

where:

$$\begin{pmatrix} t(\theta) \\ h(\theta) \end{pmatrix} = \begin{bmatrix} B(\mathcal{B}, \theta) & -B'(\mathcal{B}, \theta) \\ B'(\mathcal{B}, \theta) & B(\mathcal{B}, \theta) \end{bmatrix} \cdot \begin{pmatrix} \cos(\theta) \\ \sin(\theta) \end{pmatrix}. \quad (3.7)$$

Proof: See Huseby et al. (2015a) ■

The function $B(\mathcal{B}, \cdot)$ introduced in (3.3) can be extended to a function defined for all $\theta \in \mathbb{R}$. Since the trigonometric functions $\cos(\cdot)$ and $\sin(\cdot)$ are periodic, the extended version of $B(\mathcal{B}, \cdot)$ is periodic as well and have the property that $B(\mathcal{B}, \theta) = B(\mathcal{B}, \theta \pm 2n\pi)$ for all $n \in \mathbb{N}$. Since the set \mathcal{B} is convex, the function $B(\mathcal{B}, \cdot)$ must satisfy a certain condition. In order to investigate this further we assume that the $B(\mathcal{B}, \cdot)$ is two times differentiable, and consider the derivative of $(t(\theta), h(\theta))$ with respect to θ . By (3.7) we get that:

$$\begin{aligned} t'(\theta) &= B'(\mathcal{B}, \theta) \cos(\theta) - B(\mathcal{B}, \theta) \sin(\theta) \\ &\quad - B''(\mathcal{B}, \theta) \sin(\theta) - B'(\mathcal{B}, \theta) \cos(\theta) \\ &= -[B(\mathcal{B}, \theta) + B''(\mathcal{B}, \theta)] \sin(\theta) \\ h'(\theta) &= B''(\mathcal{B}, \theta) \cos(\theta) - B'(\mathcal{B}, \theta) \sin(\theta) \\ &\quad + B'(\mathcal{B}, \theta) \sin(\theta) + B(\mathcal{B}, \theta) \cos(\theta) \\ &= [B(\mathcal{B}, \theta) + B''(\mathcal{B}, \theta)] \cos(\theta). \end{aligned}$$

That is, we have:

$$\begin{pmatrix} t'(\theta) \\ h'(\theta) \end{pmatrix} = [B(\mathcal{B}, \theta) + B''(\mathcal{B}, \theta)] \cdot \begin{pmatrix} -\sin(\theta) \\ \cos(\theta) \end{pmatrix}. \quad (3.8)$$

In order to prove the convexity condition for $B(\mathcal{B}, \cdot)$, we need the following lemmas:

Lemma 3.9 *Let $\mathcal{B} \subset \mathbb{R}^2$ be a compact and strictly convex set, and let:*

$$\tilde{\mathcal{B}} = \{(\tilde{t}, \tilde{h}) = (t - t_0, h - h_0) : (t, h) \in \mathcal{B}\} \quad (3.9)$$

for some point $(t_0, h_0) \in \mathbb{R}^2$. Then $B(\tilde{\mathcal{B}}, \theta)$ is given by:

$$B(\tilde{\mathcal{B}}, \theta) = B(\mathcal{B}, \theta) - t_0 \cos(\theta) - h_0 \sin(\theta),$$

for all $\theta \in \mathbb{R}$. Moreover, assuming that $B(\mathcal{B}, \cdot)$ is two times differentiable, we have:

$$\begin{aligned} B'(\tilde{\mathcal{B}}, \theta) &= B'(\mathcal{B}, \theta) + t_0 \sin(\theta) - h_0 \cos(\theta), \\ B''(\tilde{\mathcal{B}}, \theta) &= B''(\mathcal{B}, \theta) + t_0 \cos(\theta) + h_0 \sin(\theta). \end{aligned}$$

Proof: By (3.3) we have:

$$\begin{aligned}
B(\tilde{\mathcal{B}}, \theta) &= \sup_{(\tilde{t}, \tilde{h}) \in \tilde{\mathcal{B}}} \{\tilde{t} \cos(\theta) + \tilde{h} \sin(\theta)\} \\
&= \sup_{(t, h) \in \mathcal{B}} \{(t - t_0) \cos(\theta) + (h - h_0) \sin(\theta)\} \\
&= \sup_{(t, h) \in \mathcal{B}} \{t \cos(\theta) + h \sin(\theta)\} - t_0 \cos(\theta) - h_0 \sin(\theta) \\
&= B(\mathcal{B}, \theta) - t_0 \cos(\theta) - h_0 \sin(\theta)
\end{aligned}$$

The remaining parts of the lemma follow by taking derivatives ■

Lemma 3.10 *Let $\mathcal{B} \subset \mathbb{R}^2$ be a compact and strictly convex set, and assume that $B(\mathcal{B}, \cdot)$ is two times differentiable. Then there exists a $\theta_0 \in (0, 2\pi)$ such that:*

$$B(\mathcal{B}, \theta_0) + B''(\mathcal{B}, \theta_0) > 0.$$

Proof: Let (t_0, h_0) be an interior point of \mathcal{B} and let $\tilde{\mathcal{B}}$ be defined as in (3.9). Then we have:

$$t_0 \cos(\theta) + h_0 \sin(\theta) < B(\mathcal{B}, \theta) \quad \text{for all } \theta \in [0, 2\pi)$$

Hence, by Lemma 3.9 we have:

$$B(\tilde{\mathcal{B}}, \theta) = B(\mathcal{B}, \theta) - t_0 \cos(\theta) - h_0 \sin(\theta) > 0 \quad \text{for all } \theta \in [0, 2\pi)$$

Moreover, since $B(\tilde{\mathcal{B}}, \theta)$ extended to a function defined for all $\theta \in \mathbb{R}$, is periodic, it follows that the extended version of $B'(\tilde{\mathcal{B}}, \theta)$ is periodic as well. In particular that $B'(\tilde{\mathcal{B}}, 0) = B'(\tilde{\mathcal{B}}, 2\pi)$. Hence, by the mean value theorem, there exists a $\theta_0 \in (0, 2\pi)$ such that $B''(\tilde{\mathcal{B}}, \theta_0) = 0$. From this it follows that:

$$B(\tilde{\mathcal{B}}, \theta_0) + B''(\tilde{\mathcal{B}}, \theta_0) > 0$$

By Lemma 3.9 we also that:

$$\begin{aligned}
B(\tilde{\mathcal{B}}, \theta_0) + B''(\tilde{\mathcal{B}}, \theta_0) &= B(\mathcal{B}, \theta_0) - t_0 \cos(\theta_0) - h_0 \sin(\theta_0) \\
&\quad + B''(\mathcal{B}, \theta_0) + t_0 \cos(\theta_0) + h_0 \sin(\theta_0) \\
&= B(\mathcal{B}, \theta_0) + B''(\mathcal{B}, \theta_0),
\end{aligned}$$

and thus, the result follows ■

As θ runs through $[0, 2\pi)$, the point $(t(\theta), h(\theta))$ runs counterclockwise through the boundary $\partial\mathcal{B}$. The derivative $(t'(\theta), h'(\theta))$ is the tangent vector to $\partial\mathcal{B}$ at $(t(\theta), h(\theta))$.

Since the set \mathcal{B} is assumed to be strictly convex, the angle between $(t'(\theta), h'(\theta))$ and $(t'(\theta + \Delta), h'(\theta + \Delta))$ is positive for any $\theta \in [0, 2\pi)$ and small $\Delta > 0$. We then define:

$$\mathbf{v}(\theta) = (t'(\theta), h'(\theta), 0), \quad \theta \in [0, 2\pi),$$

and calculate the cross-product:

$$\begin{aligned}
\mathbf{v}(\theta) \times \mathbf{v}(\theta + \Delta) &= \begin{vmatrix} \mathbf{i} & \mathbf{j} & \mathbf{k} \\ t'(\theta) & h'(\theta) & 0 \\ t'(\theta + \Delta) & h'(\theta + \Delta) & 0 \end{vmatrix} \\
&= (0, 0, t'(\theta) \cdot h'(\theta + \Delta) - h'(\theta) \cdot t'(\theta + \Delta))
\end{aligned}$$

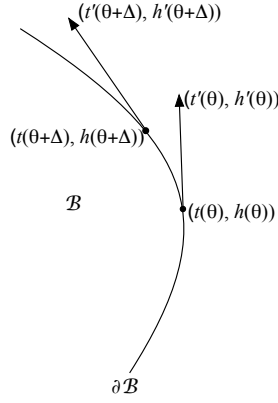


Figure 3.2: Derivatives

By the *right-hand rule* of the cross-product the angle between the vectors $(t'(\theta), h'(\theta), 0)$ and $(t'(\theta + \Delta), h'(\theta + \Delta), 0)$ is positive if and only if:

$$t'(\theta) \cdot h'(\theta + \Delta) - h'(\theta) \cdot t'(\theta + \Delta) > 0.$$

Inserting the expressions for the derivatives given in (3.8) we get:

$$\begin{aligned} & t'(\theta) \cdot h'(\theta + \Delta) - h'(\theta) \cdot t'(\theta + \Delta) \\ &= [B(\mathcal{B}, \theta) + B''(\mathcal{B}, \theta)] \cdot [B(\mathcal{B}, \theta + \Delta) + B''(\mathcal{B}, \theta + \Delta)] \\ &\quad \cdot (-\sin(\theta) \cos(\theta + \Delta) + \sin(\theta + \Delta) \cos(\theta)) \\ &= [B(\mathcal{B}, \theta) + B''(\mathcal{B}, \theta)] \cdot [B(\mathcal{B}, \theta + \Delta) + B''(\mathcal{B}, \theta + \Delta)] \cdot \sin(\Delta). \end{aligned}$$

Since $\Delta > 0$ is small, we have $\sin(\Delta) > 0$. Hence, the angle between $(t'(\theta), h'(\theta))$ and $(t'(\theta + \Delta), h'(\theta + \Delta))$ is positive if and only if:

$$[B(\mathcal{B}, \theta) + B''(\mathcal{B}, \theta)] \cdot [B(\mathcal{B}, \theta + \Delta) + B''(\mathcal{B}, \theta + \Delta)] > 0$$

for all $\theta \in [0, 2\pi)$ and small $\Delta > 0$. This condition holds if and only if the sign of $B(\mathcal{B}, \theta) + B''(\mathcal{B}, \theta)$ is the same for all $\theta \in [0, 2\pi)$.

By Lemma 3.10 there exists at least one $\theta_0 \in (0, 2\pi)$ such that $B(\mathcal{B}, \theta_0) + B''(\mathcal{B}, \theta_0) > 0$. Hence, we have shown the following important result:

Theorem 3.11 *Let $\mathcal{B} \subset \mathbb{R}^2$ be a compact and strictly convex set, and assume that $B(\mathcal{B}, \cdot)$ is two times differentiable. Then we have:*

$$B(\mathcal{B}, \theta) + B''(\mathcal{B}, \theta) > 0 \text{ for all } \theta \in [0, 2\pi). \quad (3.10)$$

Given a periodic function which does not satisfy (3.10), it is very easy to modify this function so that the condition is satisfied. The following result shows how this can be done.

Proposition 3.12 *Let $C(\cdot)$ be a periodic function with period 2π which is two times differentiable. Assuming that both C and C'' are bounded, there exists a constant C_0 such that the function $\tilde{C}(\cdot) = C_0 + C(\cdot)$ satisfies (3.10).*

Proof: We let:

$$c = \inf_{\theta \in [0, 2\pi)} [C(\theta) + C''(\theta)]$$

Since both C and C'' are bounded, c must be finite. If $c > 0$, $C(\cdot)$ satisfies (3.10). We may then let $C_0 = 0$. Hence, $\tilde{C}(\cdot) = C(\cdot)$, and thus, $\tilde{C}(\cdot)$ obviously satisfies (3.10) as well. On the other hand, if $c \leq 0$, we let C_0 be some number greater than $-c$. Since $\tilde{C}'' = C''$, it follows that for all $\theta \in [0, 2\pi)$ we have:

$$\begin{aligned} \tilde{C}(\theta) + \tilde{C}''(\theta) &= C_0 + C(\theta) + C''(\theta) \\ &> -c + C(\theta) + C''(\theta) \\ &\geq -c + c = 0. \end{aligned}$$

Hence, we conclude that $\tilde{C}(\cdot)$ satisfies (3.10) ■

3.1 Valid convex environmental contours

We now turn to the problem of finding a convex contour $\partial\mathcal{B}$ which is *valid*, i.e., a contour that has an exceedance probability which is less than or equal to a given target probability $p_e \in (0, 0.5)$.

Following Huseby et al. (2015a) we let $C(\theta)$ be defined for all angles $\theta \in [0, 2\pi)$ as:

$$C(\theta) = \inf\{y : P[Y(\theta) > y] \leq p_e\}, \quad (3.11)$$

where $Y(\theta) = T \cos(\theta) + H \sin(\theta)$. The function C is referred to as the p_e -level *percentile function* of the joint distribution of (T, H) .

For $\theta \in [0, 2\pi)$ we also introduce :

$$\begin{aligned} \Pi(\theta) &= \{(t, h) : t \cos(\theta) + h \sin(\theta) = C(\theta)\} \\ \Pi^+(\theta) &= \{(t, h) : t \cos(\theta) + h \sin(\theta) \geq C(\theta)\}, \\ \Pi^-(\theta) &= \{(t, h) : t \cos(\theta) + h \sin(\theta) \leq C(\theta)\}. \end{aligned}$$

By the definition of $C(\theta)$ and the assumption that the distribution of (T, H) is absolutely continuous with respect to the Lebesgues measure in \mathbb{R}^2 it follows that for all $\theta \in [0, 2\pi)$ we have:

$$\begin{aligned} P[(T, H) \in \Pi^+(\theta)] &= P[T \cos(\theta) + H \sin(\theta) \geq C(\theta)] \\ &= P[T \cos(\theta) + H \sin(\theta) > C(\theta)] = p_e \end{aligned}$$

If we can find a convex set \mathcal{B} such that $B(\mathcal{B}, \theta) \geq C(\theta)$, it follows by Proposition 3.3 that:

$$\begin{aligned} P_e(\mathcal{B}, \mathcal{E}) &= \sup_{\theta \in [0, 2\pi)} \{P[(T, H) \in \Pi^+(\mathcal{B}, \theta)]\} \\ &= \sup_{\theta \in [0, 2\pi)} \{P[T \cos(\theta) + H \sin(\theta) \geq B(\mathcal{B}, \theta)]\} \\ &\leq \sup_{\theta \in [0, 2\pi)} \{P[T \cos(\theta) + H \sin(\theta) \geq C(\theta)]\} = p_e \end{aligned}$$

Hence, this implies that $\partial\mathcal{B}$ is a valid environmental contour. As stated Section 2 our goal is to find a *minimal* set \mathcal{B} such that $\partial\mathcal{B}$ is valid. By Proposition 3.4 this means that we want $B(\mathcal{B}, \theta)$ to be as small as possible. Thus, if there exists a compact and convex set \mathcal{B} such that $B(\mathcal{B}, \theta) = C(\theta)$ for all $\theta \in [0, 2\pi)$, this set will be the minimal compact and convex set with the property that $\partial\mathcal{B}$ is a valid environmental contour. The following result summarizes the consequences of all these findings:

Theorem 3.13 *Let $C(\cdot)$ be defined by (3.11), and assume that there exists a compact and convex set \mathcal{B} such that $B(\mathcal{B}, \theta) = C(\theta)$ for all $\theta \in [0, 2\pi)$. Then \mathcal{B} is the minimal compact and convex set with the property that $\partial\mathcal{B}$ is a valid environmental contour, and the set \mathcal{B} is given by:*

$$\mathcal{B} = \bigcap_{\theta \in [0, 2\pi)} \Pi^-(\theta) \quad (3.12)$$

If \mathcal{B} is strictly convex, and $C(\cdot)$ is differentiable, the environmental contour, $\partial\mathcal{B}$, can be expressed as:

$$\partial\mathcal{B} = \{(t(\theta), h(\theta)) : \theta \in [0, 2\pi)\},$$

where:

$$\begin{pmatrix} t(\theta) \\ h(\theta) \end{pmatrix} = \begin{bmatrix} C(\theta) & -C'(\theta) \\ C'(\theta) & C(\theta) \end{bmatrix} \cdot \begin{pmatrix} \cos(\theta) \\ \sin(\theta) \end{pmatrix}, \quad (3.13)$$

If $C(\cdot)$ is two times differentiable, a necessary condition for the existence of a strictly convex set \mathcal{B} such that $B(\mathcal{B}, \theta) = C(\theta)$ for all $\theta \in [0, 2\pi)$ is that:

$$C(\theta) + C''(\theta) > 0 \text{ for all } \theta \in [0, 2\pi). \quad (3.14)$$

Note that the function $C(\cdot)$ is determined by the joint distribution of T and H . It is possible to construct distributions where $C(\cdot)$ does not satisfy (3.14). In such cases the contour defined by the formula (3.13), will not be the boundary of a convex set. When this happens, $C(\cdot)$ must be adjusted. We will return to this issue in Section 5.

In this section we have studied environmental contours defined through the p_e -level percentile function (3.11). Theorem 3.13 shows that if a minimal valid environmental contour exists (for some given joint distribution of (T, H)), then it is necessarily given by the representation (3.13), and that the differential inequality (3.14) has to hold. In Section 5 we will see that this condition (3.14) is useful for analysing and improving numerical methods for constructing environmental contours. This is also true in higher dimensions, i.e. when instead of $(T, H) \in \mathbb{R}^2$ one considers a random variable in \mathbb{R}^n . By studying the connection between environmental contours and Voronoi cells, Hafver et al. (2020) proved the n -dimensional analog of (3.13) and a slightly weaker alternative of the necessary condition (3.14) (corresponding to \geq in (3.14)). This method is also discussed further in Section 4 and Section 5.

4 Estimating environmental contours

In a given practical situation the C -function is typically estimated pointwise using Monte Carlo simulations. Following Huseby et al. (2015a) we assume that we have a sample from the joint distribution of (T, H) generated using Monte Carlo simulation:

$$(T_1, H_1), \dots, (T_n, H_n)$$

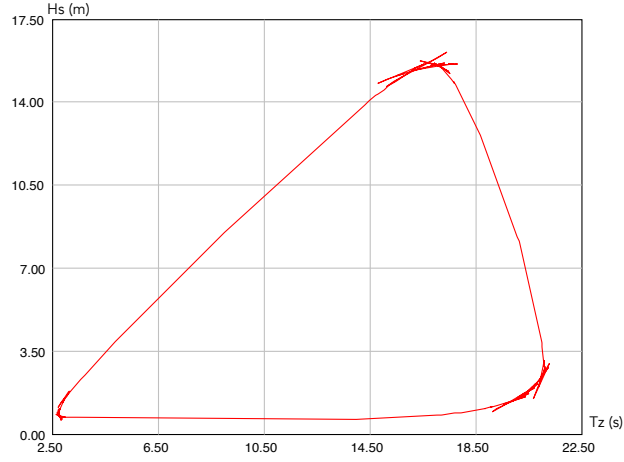


Figure 4.1: 1000 simulations, $n = 90$.

For a given angle $\theta \in [0, 2\pi)$ we calculate the projections of these points onto the unit vector $(\cos(\theta), \sin(\theta))$, i.e.:

$$Y_i(\theta) = T_i \cos(\theta) + H_i \sin(\theta), \quad i = 1, \dots, n$$

These projections are then sorted in ascending order:

$$Y_{(1)}(\theta) \leq Y_{(2)}(\theta) \leq \dots \leq Y_{(n)}(\theta).$$

Assuming that $k \leq n$ is an integer such that:

$$\frac{k}{n} \approx 1 - p_e,$$

it follows that $C(\theta)$ can be estimated by:

$$\hat{C}(\theta) = Y_{(k)}(\theta) \tag{4.1}$$

Proceeding in this fashion the C -function can be estimated for a suitable set of angles $\theta_1, \dots, \theta_n \in [0, \pi)$. We let $\hat{C}(\theta_1), \dots, \hat{C}(\theta_n)$ denote the resulting estimates. The set \mathcal{B} given in (3.12) of Theorem 3.13 can then be approximated by a polygon of the following form:

$$\hat{\mathcal{B}} = \bigcap_{i=1}^n \hat{\Pi}^-(\theta_i), \tag{4.2}$$

where:

$$\hat{\Pi}^-(\theta_i) = \{(t, h) : t \cos(\theta) + h \sin(\theta) \leq \hat{C}(\theta_i)\}$$

There are several methods for constructing an estimate of the boundary of the set \mathcal{B} . One method is based directly on the polygon given in (4.2), where the corners are determined by computing the intersection between the hyperplanes $\Pi(\theta_i)$ and $\Pi(\theta_{i+1})$, for $i = 1, \dots, n$, and where we define $\Pi(\theta_{n+1})$ to be equal to $\Pi(\theta_1)$. This method is also similar to the method suggested by Ottesen and Aarstein (2006), and is the method used in the remaining part of

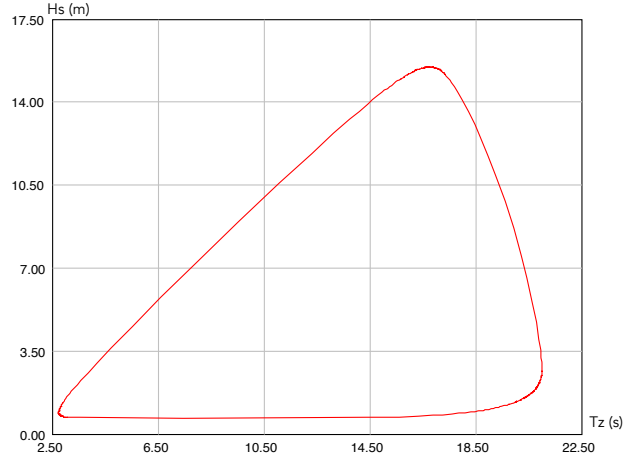


Figure 4.2: 1000000 simulations, $n = 360$.

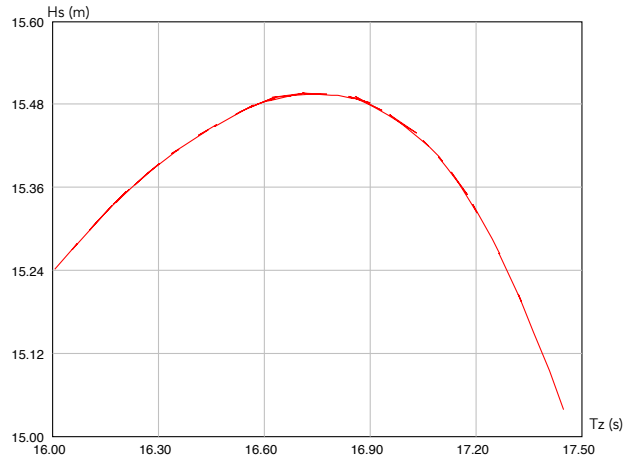


Figure 4.3: 1000000 simulations, $n = 360$.

the present paper. Another method is based on (3.13) given in Theorem 3.13. This method uses the estimate of the p_e -level percentile function given in (4.1). Other methods include the use of Fourier series and splines. For more details on this see Huseby et al. (2015a).

In Figure 4.1 the set \mathcal{B} is estimated using only a few simulations and halfspaces. We observe that the resulting contour has significant irregularities especially in the areas where the direction of the contour changes a lot. By increasing the number of simulations and halfspaces, a smoother contour is obtained. This is illustrated in Figure 4.2. If we zoom in on the border of $\hat{\mathcal{B}}$, we still find substantial "irregularities" as is seen in Figure 4.3. This issue is illustrated in a simplified way in Figure 4.4 and Figure 4.5. Figure 4.4 represents an ideal case where all the hyperplanes support \mathcal{B} . In such cases \mathcal{B} is well approximated by the polygon obtained as the intersection of the corresponding halfspaces. The corners of the polygon are obtained as the intersection points between successive hyperplanes, and the boundary of the polygon is obtained by drawing straight lines between the corners. Since all the hyperplanes support \mathcal{B} , no loops occur. Figure 4.5 on the other hand represents a case where at least one of the hyperplanes does not support \mathcal{B} . Attempting to obtain

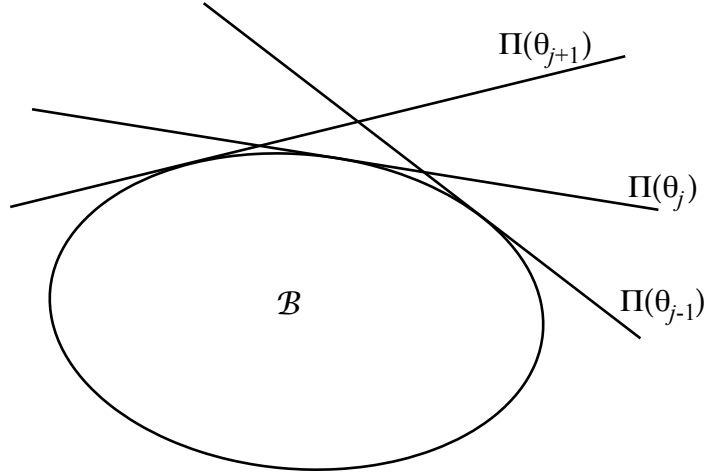


Figure 4.4: Ideal case: All hyperplanes support \mathcal{B}

the boundary of the polygon by drawing straight lines between the intersection points will result in a loop. Moreover, if we use the intersection of the halfspaces as our set \mathcal{B} , this set will typically have a slightly higher exceedance probability than the desired value p_e .

Hafver et al. (2020) has shown that the polygon given by (4.2) corresponds to the Voronoi cell of a point $\mathbf{o} = (o_x, o_y) \in \hat{\mathcal{B}}$ with respect to the function

$$s^{\mathbf{o}}(\theta) = \begin{pmatrix} o_x \\ o_y \end{pmatrix} + 2C^{\mathbf{o}}(\theta) \begin{pmatrix} \cos(\theta) \\ \sin(\theta) \end{pmatrix}, \quad (4.3)$$

where

$$C^{\mathbf{o}}(\theta) = C(\theta) - \begin{pmatrix} o_x \\ o_y \end{pmatrix} \cdot \begin{pmatrix} \cos(\theta) \\ \sin(\theta) \end{pmatrix}. \quad (4.4)$$

This means that

$$\hat{\mathcal{B}} = \text{Vor}(\mathbf{o}, \mathcal{S}) = \left\{ \mathbf{x} \in \mathbb{R}^n \mid \|\mathbf{x} - \mathbf{o}\| \leq \inf_{\mathbf{s} \in \mathcal{S}} \|\mathbf{x} - \mathbf{s}\| \right\}, \quad (4.5)$$

where $\mathcal{S} = \{s^{\mathbf{o}}(\theta) \mid \theta \in [0, 2\pi)\}$. This suggests an alternative approach to construct environmental contours, by computing the above Voronoi cell based on estimated values of $C(\theta)$. The Voronoi approach can also be used to detect hyperplanes that do not support \mathcal{B} , as the corresponding points in \mathcal{S} will not be connected to \mathbf{o} in the dual Delaunay triangulation. For further details see (Hafver et al., 2020).

5 Constructing a smooth environmental contour

In this section we will show how the loops illustrated in the previous sections can be removed. We demonstrate the method by considering a specific example. In this example we let $p_e = 1.37 \cdot 10^{-5}$, which corresponds to a return period of 25 years and a data collection rate of 8 observations per day.

The joint long-term models for *significant wave height*, denoted by H , and *wave period* denoted by T is given by:

$$f_{T,H}(t, h) = f_H(h) f_{T|H}(t|h)$$

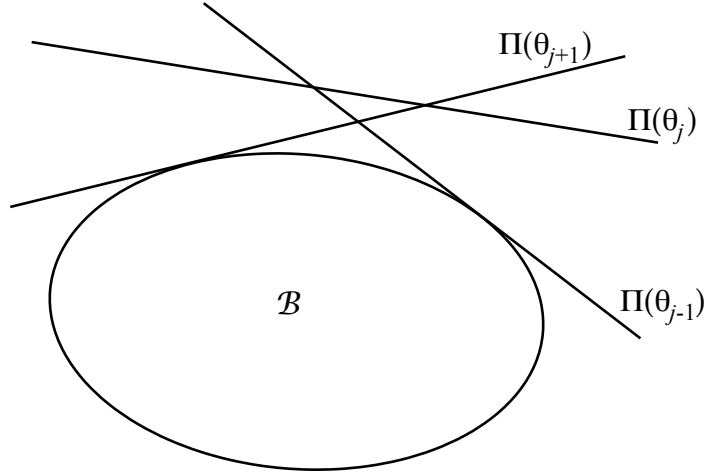


Figure 4.5: Irregular case: The hyperplane $\Pi(\theta_j)$ does *not* support \mathcal{B}

α	β	γ
2.259	1.285	0.701

Table 5.1: Fitted parameter for the three-parameter Weibull distribution

where a three-parameter Weibull distribution is used for the significant wave height, H , and a lognormal conditional distribution is used for the wave period, T .

The Weibull distribution is parameterized by a location parameter, γ , a scale parameter α , and a shape parameter β :

$$f_H(h) = \frac{\beta}{\alpha} \left(\frac{h - \gamma}{\alpha} \right)^{\beta-1} e^{-[(h-\gamma)/\alpha]^\beta}, \quad h \geq \gamma.$$

The lognormal distribution has two parameters, the log-mean μ and the log-standard deviation σ and is expressed as:

$$f_{T|H}(t|h) = \frac{1}{t\sqrt{2\pi}} e^{-[(\ln(t)-\mu)^2/(2\sigma^2)]}, \quad t \geq 0,$$

The dependence between H and T is modelled by letting the parameters μ and σ be expressed in terms of H as follows:

$$\begin{aligned} \mu &= E[\ln(T)|H = h] = a_1 + a_2 h^{a_3}, \\ \sigma &= SD[\ln(T)|H = h] = b_1 + b_2 e^{b_3 h}. \end{aligned}$$

The parameters are estimated using available data from the relevant geographical location and are listed in Table 5.1 and Table 5.2.

The resulting environmental contour, based on 1 million simulations, importance sampling and $n = 360$ hyperplanes, is illustrated in Figure 5.1. While this contour may appear to be very smooth, it turns out that is not at all the case.

In order to show this we measure the angle between successive sides of the polygon. For a convex polygon, these angles should all be non-negative. In the simple polygon with just

	$i = 1$	$i = 2$	$i = 3$
a_i	1.069	0.898	0.243
b_i	0.025	0.263	-0.148

Table 5.2: Fitted parameter for the conditional log-normal distribution

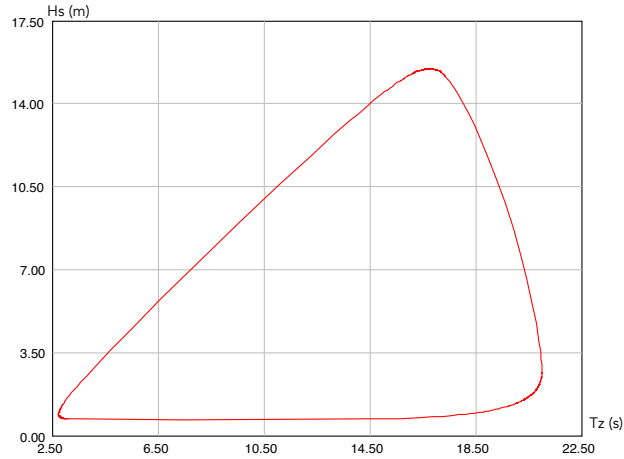


Figure 5.1: Environmental contour before smoothing.

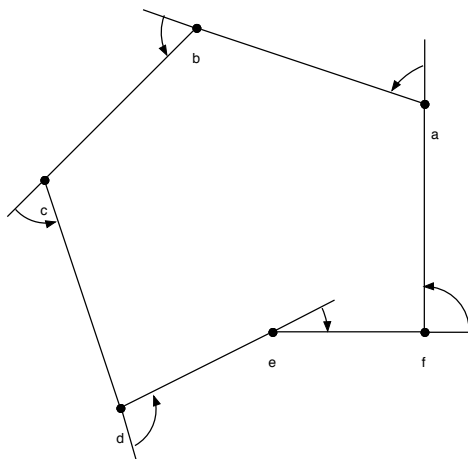


Figure 5.2: Measuring polygon angles

six corners shown in Figure 5.2 we observe that all angles are positive except the angle at corner e . As a result the polygon is clearly not convex.

In Figure 5.3 we have plotted the angles found at the 360 corners of the contour shown in Figure 4.2. Due to a high number of loops in some areas we see that a substantial number of the angles are indeed negative.

Since the estimated environmental contours shown here are polygons, these sets are clearly not strictly convex. Still it turns out the loop issue is strongly connected to the necessary condition for strict convexity given in (3.14) in Theorem 3.13. In order to study this further we have estimated values of $C(\theta) + C'''(\theta)$ using interpolation and plotted the resulting curve in Figure 5.4. We observe that the curve values are mostly positive except

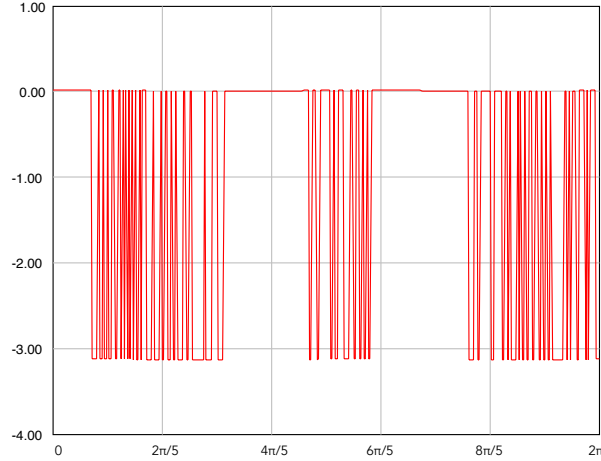


Figure 5.3: Polygon angles (radians) of the environmental contour before smoothing.

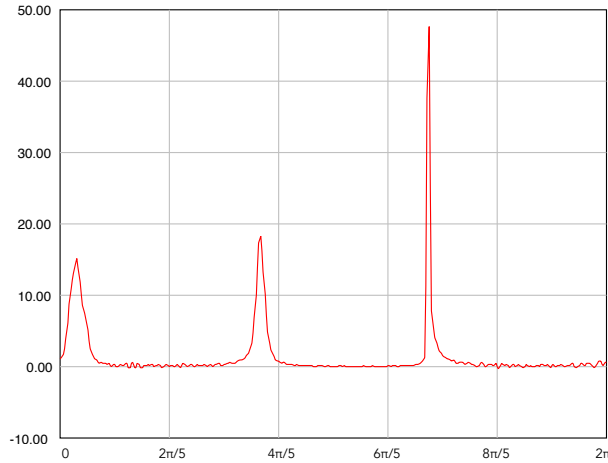


Figure 5.4: $C(\theta) + C''(\theta)$ before smoothing.

for some clusters of small negative values. It is these negative values that cause the loops.

By Proposition 3.12 it follows that if C is a known function, a convex set can always be constructed by increasing this function by a suitable positive constant. It is possible to prove that a similar effect occurs for the estimated C -function. If we add a sufficiently large positive constant to this function, the intersection points between the hyperplanes will be more spread out. As a result all the loops disappear. However, this change also inflates the contour considerably, which is usually not desirable. In the following we have chosen a different approach. By considering the plot it is evident that the issue with loops appears to be caused mostly by estimation errors. Fortunately, this problem can be remedied by applying a modest amount of smoothing. Thus, to get rid of the loops along the contour, we simply use a smoothed version of the estimated C -curve. A simple smoothing formula utilizing information from nearby points could e.g. be the following:

$$\tilde{C}(\theta_j) = \frac{\sum_{i=-k}^{+k} \omega_i C(\theta_{j+i})}{\sum_{i=-k}^{+k} \omega_i}, \quad j = 1, \dots, n,$$

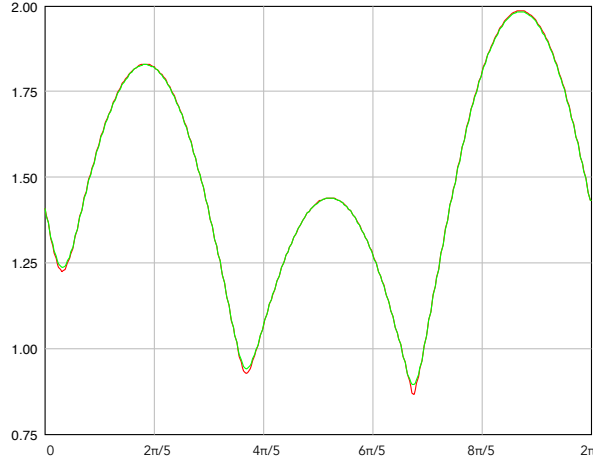


Figure 5.5: Unsmoothed $C(\theta)$ (red curve) versus smoothed $C(\theta)$ (green curve)

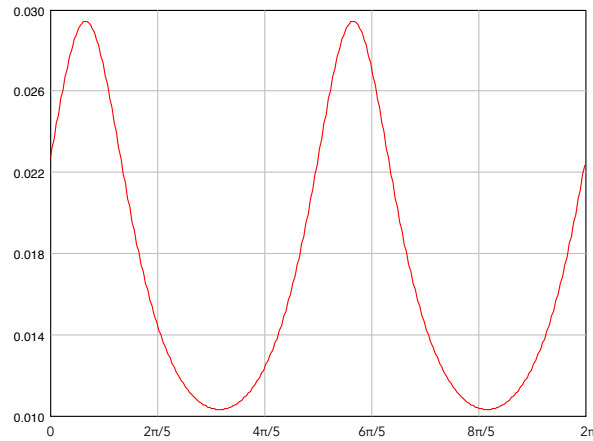


Figure 5.6: Polygon angles (radians) of the environmental contour after smoothing.

where $k \geq 0$ is a suitable integer determining the number of utilized nearby points. Moreover, $\omega_{-k}, \dots, \omega_{+k}$ are suitable weights determining the influence of the nearby points. In the above formula the indices are "looped", so that $\theta_{n+i} = \theta_i$, $i = 1, 2, \dots, k$, while $\theta_{1-i} = \theta_{n+1-i}$, $i = 1, 2, \dots, k$. In our calculations we have used $k = 5$ and:

$$\omega_{-i} = \omega_{+i} = (6 - k), \quad i = 0, 1, \dots, 5.$$

In Figure 5.5 we have plotted both the unsmoothed and smoothed versions of $C(\theta)$ in the same plot. With the level of smoothing applied, the two curves are almost identical except for some areas around the local minimas.

However, even this very minor adjustment has a dramatic effect on the measured angles along the contour. In Figure 5.6 we have plotted the angles after the smoothing. These angles are indeed very different from the angles shown in Figure 5.3.

In Figure 5.7 we have plotted $C(\theta) + C'''(\theta)$ after smoothing has been applied. Now all points are non-negative which by Theorem 3.11 implies that the resulting contour is convex.

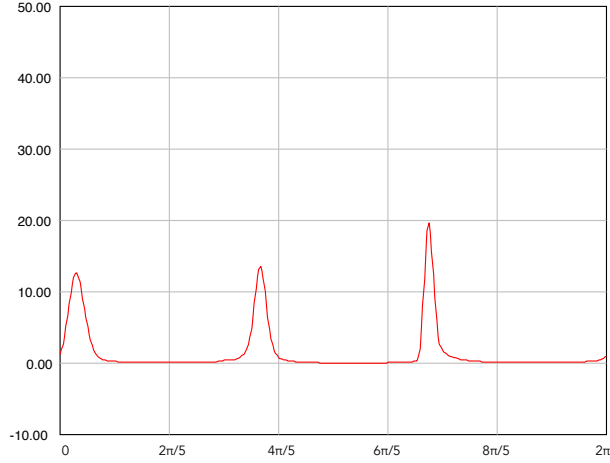


Figure 5.7: $C(\theta) + C''(\theta)$ after smoothing.

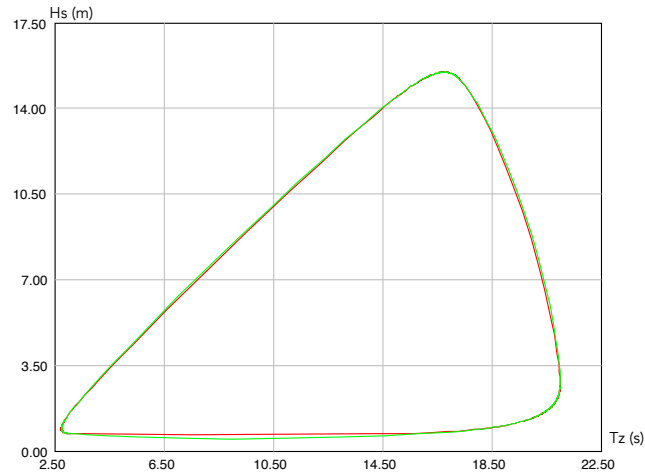


Figure 5.8: Unsmoothed contour (red curve) versus smoothed contour (green curve)

Finally, in Figure 5.8 we have plotted both the unsmoothed and smoothed contours. The two contours are apparently not very different except that the smoothed curve is somewhat more rounded. In order to avoid too strict design requirements, one wants the set \mathcal{B} to be as small as possible. We observe that the set bounded by the smoothed contour is slightly larger than set bounded by the unsmoothed contour. On the other hand, by using the smoothed curve, we get a contour with a more precise exceedance probability, which after all is the most important goal.

The method described above constructs a convex environmental contour by first smoothing $C(\theta)$. An alternative method to obtain valid environmental contour is described in Hafver et al. (2020), where a Voronoi contour is computed based on the un-smoothed/raw $C(\theta)$ and this contour is then projected outwards on the hyperplanes $\hat{\Pi}(\theta_i)$ included in (4.2).

6 Conclusions

In the present paper we have focused on convex environmental contours, and studied various properties of such contours. By establishing a mapping between angles $\theta \in [0, 2\pi)$ and the points along the contour, we have shown that such contours can be parametrized. The mapping is valid whenever the contour set is strictly convex. A necessary condition for strict convexity is also proved. Using Monte Carlo simulations we can estimate convex environmental contours which in principle have a constant exceedance probability in all tail directions. Due to numerical instabilities, however, such contours typically contain small irregularities or loops. The presence of such loops is closely related to the necessary conditions for strict convexity. By examining how this condition is violated in areas with loops, it becomes clear that the problem can be eliminated by a simple smoothing scheme. This method is demonstrated on a specific numerical example.

References

- Baarholm, G. S., S. Haver, and O. D. Økland (2010). Combining contours of significant wave height and peak period with platform response distributions for predicting design response. *Marine Structures* 23, 147–163.
- Ditlevsen, O. (2002). Stochastic model for joint wave and wind loads on offshore structures. *Structural Safety* 24, 139–163.
- Hafver, A., C. Agrell, and E. Vanem (2020). Environmental contours as Voronoi cells. *arXiv e-prints*, arXiv:2008.13480.
- Haver, S. (1987). On the joint distribution of heights and periods of sea waves. *Ocean Engineering* 14, 359–376.
- Haver, S. and S. R. Winterstein (2009). Environmental contour lines: A method for estimating long term extremes by a short term analysis. *Transactions of the Society of Naval Architects and Marine Engineers* 116, 116–127.
- Huseby, A. B., E. Vanem, and B. Natvig (2013). A new approach to environmental contours for ocean engineering applications based on direct Monte Carlo simulations. *Ocean Engineering* 60, 124–135.
- Huseby, A. B., E. Vanem, and B. Natvig (2015a). Alternative environmental contours for structural reliability analysis. *Structural Safety* 54, 32–45.
- Huseby, A. B., E. Vanem, and B. Natvig (2015b). A new Monte Carlo method for environmental contour estimation. In T. Nowakowski, M. Młyńczak, A. Jodejko-Pietruczuk, and S. Werbińska-Wojciechowska (Eds.), *Safety and Reliability: Methodology and Applications, Proceedings of the European safety and reliability Conference*, pp. 2091–2098. Taylor & Francis.
- Jonathan, P., K. Ewans, and J. Flynn (2011). On the estimation of ocean engineering design contours. In *Proc. 30th International Conference on Offshore Mechanics and Arctic Engineering*, pp. 1–8.

- Moan, T. (2009). Development of accidental collapse limit state criteria for offshore structures. *Structural Safety* 31, 124–135.
- Ottesen, T. and J. A. Aarstein (2006). The statistical boundary polygon of a two parameter stochastic process. In *Proc. 25th International Conference on Offshore Mechanics and Arctic Engineering*, pp. 1–6.
- Rosenblatt, M. (1952). Remarks on a multivariate transformation. *The Annals of Mathematical Statistics* 23, 470–472.
- Winterstein, S. R., T. C. Ude, C. A. Cornell, P. Bjerager, and S. Haver (1993). Environmental parameters for extreme response: Inverse form with omission factors. In *Proc. 6th International Conference on Structural Safety and Reliability*, pp. 551–557.